

# H1320+551: A Seyfert 1.8/1.9 galaxy with an unabsorbed X-ray spectrum<sup>★</sup>

X. Barcons, F.J. Carrera, M.T. Ceballos

*Instituto de Física de Cantabria (CSIC-UC), 39005 Santander, Spain*

September 2002

## ABSTRACT

We present new optical spectroscopic and XMM-Newton X-ray observations of the Active Galactic Nucleus H1320+551. The optical data (consistent with but of better quality than a previously published spectrum) show this source to be a Seyfert 1.8/1.9 galaxy at  $z = 0.0653$ . The narrow line region is significantly reddened, with a Balmer decrement  $H\alpha/H\beta \sim 6$  and the broad line region, with a barely detectable  $H\beta$  broad component, shows a much pronounced Balmer decrement ( $H\alpha/H\beta > 27$ ). In spite of this, the EPIC-pn X-ray spectrum exhibits a power-law continuum with a soft excess that is well fitted by a black body, with no photoelectric absorption above the galactic value. A Fe K emission line is also seen at a rest-frame energy  $\sim 6.5$  keV with an equivalent width of  $\sim 400$  eV, far too weak for the source being Compton-thick. Reconciling the optical and X-ray data requires the narrow line region being internally reddened but with small covering factor over the nuclear emission and the Balmer decrement of the broad line region being an intrinsic property rather than caused by reddening/absorption. The H1320+551 Seyfert 1.8/1.9 galaxy is not consistent with being an obscured Seyfert 1 nucleus, i.e., it does not match the basic AGN unified scheme hypothesis.

**Key words:** galaxies:active, Seyfert; X-rays:galaxies

## 1 INTRODUCTION

The X-ray spectral properties of Active Galactic Nuclei (AGN) are generally well correlated with their optical appearance. Seyfert 1 galaxies and QSOs have usually steep X-ray spectra with little, if any, intrinsic photoelectric absorption (Nandra & Pounds 1994). Seyfert 2 galaxies have, on the contrary, absorbed X-ray spectra (Smith & Done 1996). This is hardly surprising in the framework of the simplest version of the AGN unified model (Antonucci 1993), as the molecular gas and dust that prevents the direct view of the Broad-Line region in type 2 Seyferts (the “torus”) is likely to also contain atomic gas that will absorb soft X-rays.

Unified AGN models for the cosmic X-ray background (XRB), first suggested by Setti & Woltjer (1989) and later worked out by Madau, Ghisellini & Fabian (1994), Comastri et al (1995) and Gilli, Salvati & Hasinger (2001), make use of this feature. A broad distribution of photoelectric absorbing columns is assumed, which results in an integrated XRB with the required spectral shape. X-ray surveys are expected to reveal mostly type 1 AGN for soft unabsorbed

X-ray sources and type 2 AGN for hard absorbed X-ray sources. Indeed, soft X-ray surveys carried out with *ROSAT* are rich in type 1 AGNs and QSOs (see, e.g., Mason et al 2000 and Lehmann et al 2001 for medium and deep *ROSAT* surveys). On the contrary, hard X-ray surveys carried out with *BeppoSAX* do contain large numbers of type 2 AGN (Fiore et al 1999).

Risaliti, Maiolino & Salvati (1999) found that the X-ray absorption in a sample of [OIII]-selected type 1.8, 1.9 and 2 AGN reveals much higher absorbing columns than in samples selected by other means, a large fraction of the sources being actually Compton-thick. Since [OIII] emission is supposed to arise above the obscuring torus, [OIII] selection is likely to be an orientation-independent measure of the AGN intrinsic luminosity. Still, a rough trend of increasing X-ray absorption with AGN Seyfert type is found (Risaliti, Maiolino & Salvati 1999, Alonso-Herrero et al 1997).

However, a number of studies show that the optical obscuration to X-ray absorption relation is not as simple as predicted by the AGN unified model. A hard spectrum selection of *ROSAT* X-ray sources, which was supposed to favour absorbed X-ray sources (Page et al 2000), revealed mostly type 1 AGN, while more type 2 AGN were expected (Page et al 2001). Granato, Danese & Franceschini (1997) proposed that X-ray absorption takes place mostly in dust-

<sup>★</sup> Based partly on observations obtained with XMM-Newton, an ESA science mission with instruments and contributions directly funded by ESA member states and the USA (NASA)

free regions, below the dust sublimation radius. This will accommodate the existence of X-ray absorbed, optically unobscured type 1 AGN.

Pappa et al (2001) have found, in a sample of Seyfert 2 galaxies, some extreme cases without or with very small apparent intrinsic X-ray absorption. The apparent lack of X-ray absorption has been attributed to some of these Seyfert 2 galaxies being actually Compton-thick, in which case we would be witnessing only scattered radiation and host galaxy emission from a circumnuclear starburst below 10 keV. Bassani et al (1999) propose a three-dimensional diagnostic that would discriminate between that possibility and true lack of absorption, on the basis of a diagram displaying the equivalent width of the Fe K emission line versus the transmission  $T$  defined as the ratio between the 2-10 keV X-ray flux (supposed to measure the emission transmitted through the torus) and the reddening-corrected [OIII] flux, assumed to measure the intrinsic AGN emission. Compton-thick type 2 AGN lie invariably at the high equivalent width low transmission end. That has helped to unmask a number of puzzling Seyfert 2 galaxies apparently unabsorbed. The data quality of the *ASCA* spectrum used by Pappa et al (2001) was certainly good enough to discard a Compton-thick origin, but did not enable the discrimination between a dusty warm absorber and a genuine broad-line region free AGN.

In this paper we present new optical and X-ray observations of H1320+551. This source was discovered by HEAO-1 as part of the Modulation Collimator-Large Area Sky Survey (Wood et al 1984). The inferred 2-10 keV flux was  $\sim 2 \times 10^{-11} \text{ erg cm}^{-2} \text{ s}^{-1}$  (Ceballos & Barcons 1996), although confusion could be an issue. Remillard et al (1993) identified this X-ray source with a type 1 AGN at  $z = 0.064$  ( $RA = 13^h 22^m 49.2^s$ ,  $DEC = +54^\circ 55' 28''$ ). However, their optical spectrum was noisy and of poor spectral resolution ( $\sim 10\text{\AA}$ ) with a barely visible  $H\beta$  line.

H1320+551 was also detected in the *ROSAT* all-sky survey and identified in the *ROSAT* Bright Survey (Schwope et al 2000). The *ROSAT* PSPC count rate was  $0.23 \pm 0.024 \text{ ct/s}$ , corresponding to an absorption-corrected 0.5-2 keV flux of  $\sim (1.9 \pm 0.2) \times 10^{-12} \text{ erg cm}^{-2} \text{ s}^{-1}$ . The PSPC Hardness Ratio was  $+0.12 \pm 0.10$ . The source had therefore a moderately steep soft X-ray spectrum in the *ROSAT* band, but the small flux ratio  $S(0.5-2)/S(2-10)$  (if the 2-10 keV flux was correct) suggested absorption. *ASCA* observed H1320+551 in May 1999 and we analyze the archival data here.

In what follows we present new optical spectroscopy and XMM-Newton X-ray observations of H1320+551. Our optical data (obtained in 1998) shows this source to be a Seyfert 1.8/1.9 galaxy at  $z = 0.0653$  with a significantly reddened narrow line region (section 2). The XMM-Newton X-ray spectrum is well described by a type-1 like continuum (power-law plus black body) with no intrinsic photoelectric absorption, plus a Fe K emission line complex (section 3). In section 4 we show that the unabsorbed X-ray spectrum is inconsistent with a dust-reddening origin for the large Balmer decrement in the broad line region, which is instead more likely to be intrinsic to the broad-line clouds, contrary to the predictions of the AGN unified model.

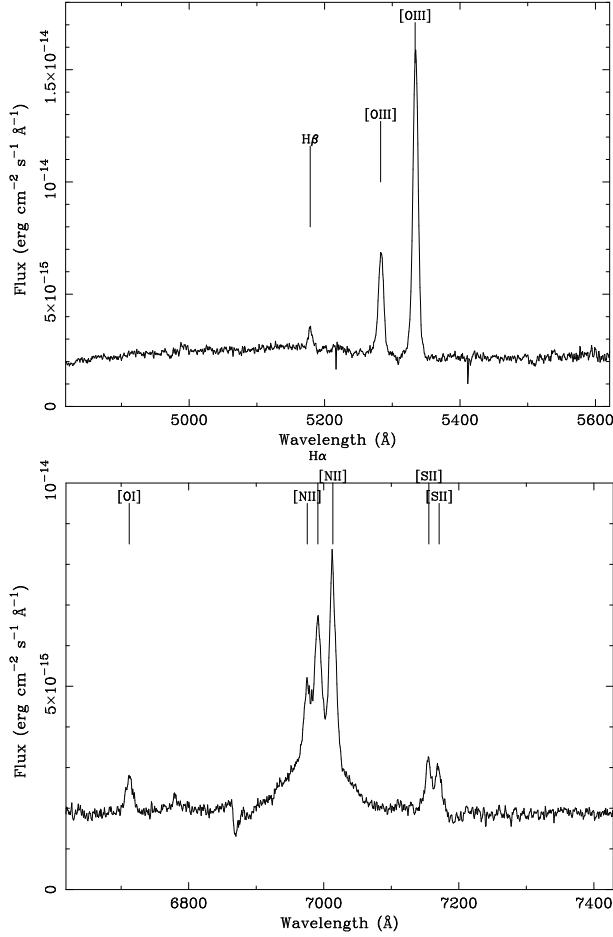
## 2 OPTICAL OBSERVATIONS

H1320+551 was observed by the 4.2m William Herschel Telescope at the Observatorio del Roque de Los Muchachos in the island of La Palma (Canary Islands, Spain), on February 26, 1998. We used the ISIS double spectrograph with 600 line/mm gratings on both the blue and red arms, with the wavelengths centered at 5200 and 7000  $\text{\AA}$  respectively, in order to observe the  $H\beta$ + [OIII] region in the blue and the  $H\alpha$ + [NII]+ [SII] in the red. During the second half of the night, when this observation was performed, the sky was clear and probably photometric. The seeing was  $\sim 1.5 \text{ arcsec}$  and we used a 1.5 arcsec slit width. Observations were carried out with the slit aligned to parallactic angle. Two exposures of 300 sec each were taken. One of the blue spectra had a cosmic ray hit on top of the  $H\beta$  line and we have not used it. The two red-arm exposures were co-added.

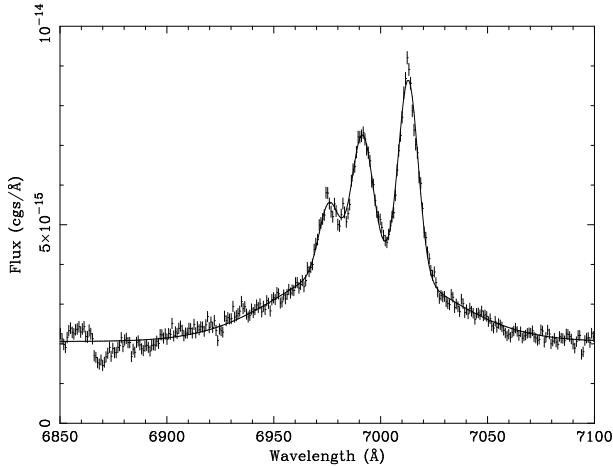
Reduction and calibration was performed according to a standard sequence under the IRAF package. It included debiasing, flat fielding, wavelength calibration with arc lamps, and flux calibration using a standard star and standard extinction curve for the observatory. The wavelength calibration gave residuals of 0.05 and 0.02  $\text{\AA}$  in the blue and in the red respectively. The measured spectral resolution (using gaussian fits to unblended arc lines) gave 2.22  $\text{\AA}$  and 2.16  $\text{\AA}$  at the central wavelengths of the blue and red channels respectively. Given the relatively poor seeing, the spectrophotometric calibration is far from accurate, but certainly good to within a factor of 2.

Fig 1 shows the resulting spectra in the blue and the red arms with marks on the most important lines. It is clear that the  $H\beta$  line is weak and dominated by a narrow component, with very weak, if any, broad component. The  $H\alpha$ + [NII] blend does, on the contrary, exhibit both a narrow and a broad  $H\alpha$  component. Therefore, according to the standard classification by Osterbrock (1981), the source is in principle a Seyfert 1.9. Remillard et al (1993) classified it as a Seyfert 1 on the basis of a low spectral resolution ( $\sim 10\text{\AA}$ ) low signal to noise optical spectrum (see fig 3 in that paper). In their spectrum the  $H\beta$  line was barely visible and the  $H\alpha$ + [NII] complex could not be deblended.

In order to measure line intensities, we selected a small portion of the spectrum around each complex and we fitted the spectrum (via  $\chi^2$  minimisation, using the *qdp* fitting routines) with a constant plus a gaussian for each putative line. Errors on the intensity of each individual wavelength channel were propagated during the reduction process, in order to perform this fit correctly. The  $H\beta$  and each one of the [OIII] doublet lines were fit independently. The [SII] doublet, slightly blended, was fitted simultaneously with two gaussians at the same redshift and with the same width. In the case of the  $H\alpha$ + [NII] blend, the 3 lines were simultaneously fitted to gaussians, all of them with the same redshift and with the additional constraint that the two [NII] lines had the same width. An additional broad  $H\alpha$  line had to be added to achieve a good fit. The result is shown in fig 2. Based on the existence of a broad  $H\alpha$  component, we searched for a corresponding  $H\beta$  one with the same velocity width. This constrained fit yields a “detection” of a weak broad  $H\beta$  component that is not required if the line width is left as a free parameter. This is the reason of the uncertainty in the 1.8/1.9 Seyfert type classification of this source.



**Figure 1.** Optical spectrum of H1320+551, blue (top) and red (bottom) arms.



**Figure 2.** Detail of the optical spectrum and fit to the  $H\alpha$ + $[NII]$  complex (see text for details)

Table 2 lists the measured line intensities and velocity widths (FWHM). These were computed from the gaussian fits, subtracting in quadrature the spectral resolution of the corresponding spectrograph channel ( $125 \text{ km s}^{-1}$  and  $100 \text{ km s}^{-1}$  in the blue and red arms respectively). The redshift that we fit to the emission lines is  $z = 0.06531 \pm 0.00002$ ,

Line	Line flux ( $\times 10^{-15} \text{ erg cm}^{-2} \text{ s}^{-1}$ )	FWHM ( $\text{km s}^{-1}$ )
H $\beta$ 4861 (narrow)	6.6	400
H $\beta$ 4861 (broad)	6.7	3710*
[OIII]4958	45.5	525
[OIII]5007	130.4	500
[OI]6300	13.5	520
[NII]6548	19.1	450
H $\alpha$ 6562 (narrow)	40.0	490
H $\alpha$ 6562 (broad)	182.9	3710
[NII]6583	56.4	450
[SII]6716	15.7	445
[SII]6730	14.4	445

**Table 1.** Measured line fluxes and velocity widths, as fitted from gaussians. A velocity of  $125 \text{ km s}^{-1}$  and of  $100 \text{ km s}^{-1}$  has been subtracted in quadrature in the blue and red arm lines respectively, to account for the spectrograph resolution. The  $H\beta$  broad line has been fit with the velocity fixed (\*) at the value found for  $H\alpha$ , as otherwise this feature is not detected.

refining the value  $z = 0.064$  reported by Remillard et al (1993).

From the line intensities we see that this AGN has significant reddening. The Balmer decrement of the Narrow Line Region (NLR), as traced by the narrow line components, is  $(H\alpha/H\beta)_{\text{NLR}} \sim 6$  (corresponding to  $E(B-V) \sim 0.5^{\text{mag}}$ ), where  $\sim 3$  is expected for a variety of models under case B recombination and optically thin NLR gas. Narrow line ratios can be reddening corrected using the Balmer decrement as the indicator. Following Baldwin, Phillips & Terlevich (1981) we find  $\log[[OIII]5007/H\beta 4861] = 1.20$  and  $\log[[NII]6583/H\alpha 6562] = 0.145$  which, as expected, place this object in the AGN zone in line diagnostic diagrams (e.g. Osterbrock 1989, fig 12.1). We have further used the measured Balmer decrement from the narrow lines ( $H\alpha/H\beta \sim 6$ ), to estimate a gas column density of  $N_H(\text{NLR}) \sim 3 \times 10^{21} \text{ cm}^{-2}$ , assuming standard gas-to-dust ratio (Bohlin et al 1978).

Since the [OIII] emission is likely to come from well above the torus, the intensity of the [OIII]5007 line is supposed to be an orientation-independent estimator of the total AGN power. Following Bassani et al (1999) and Pappa et al (2001), who use the interstellar reddening law by Savage & Mathis (1979), we estimate the unreddened [OIII]5007 flux by correcting the observed one by a factor  $[(H\alpha/H\beta)_{\text{NLR}}/3]^{2.94}$ . The resulting [OIII]5007 flux is  $\sim 1.34 \times 10^{-12} \text{ erg cm}^{-2} \text{ s}^{-1}$ .

When a similar analysis is performed in the Broad Line Region (BLR), a Balmer decrement  $(H\alpha/H\beta)_{\text{BLR}} \sim 27$  is found. This should be considered as a lower limit, as the existence of an  $H\beta$  broad component (i.e. the 1.8 Seyfert character of H1320+551) can only be established via constrained parameter fitting. If this Balmer decrement is interpreted in terms of reddening over a standard value of 3, a value of  $E(B-V)_{\text{BLR}} \sim 2^{\text{mag}}$  is found, which for a standard dust to gas ratio corresponds to a H column density of  $N_H(\text{BLR}) \sim 10^{22}$ . In the framework of the AGN unified model the difference between optical spectroscopic Seyfert types is due to an orientation effect which results in both reddening of the BLR and absorption of X-rays. Under these

circumstances the above absorption column density should be seen in the X-ray data.

We have also tried to fit the broad band optical spectra obtained here with a model mixing a reddened QSO, from the Francis et al (1991) template and a E/S0 galaxy template, from the Coleman, Wu & Weedman (1980) model. A good simultaneous description of the blue and red spectrum is achieved with the QSO template, which can accommodate a very small amount of reddening ( $E(B - V) < 0.1^{mag}$ ) but it certainly needs some host galaxy light. The latter contributes about 40-60 per cent of the optical spectrum at our reference point at 5550 Å. Significantly larger reddening over the Francis et al (1991) QSO template simply does not match the data. That suggests that whatever causes the large BLR Balmer decrement does not appear to be nuclear reddening.

### 3 PREVIOUS X-RAY OBSERVATIONS

#### 3.1 HEAO-1

As already mentioned, X-ray emission from H1320+551 was discovered in the MC-LASS survey, which assigned it a count rate of  $(4.1 \pm 0.8) \times 10^{-3}$  ct/s. Observations were carried out during 1977. Ceballos & Barcons (1996) assumed a  $\Gamma = 1.7$  power law spectrum and computed a 2-10 keV flux of  $2.0 \times 10^{-11}$  erg cm $^{-2}$  s $^{-1}$ .

#### 3.2 ROSAT

H1320+551 was detected in the *ROSAT* all-sky survey (1990/91) as source 1RXS J132248.5+545526 (Schwope et al 2000) with a PSPC count rate of  $0.23 \pm 0.024$  ct/s, and a Hardness Ratio

$$HR_{PSPC} = \frac{C(0.5 - 2.0) - C(0.1 - 0.4)}{C(0.5 - 2.0) + C(0.1 - 0.4)} = 0.12 \pm 0.10$$

where  $C(0.1 - 0.4)$  and  $C(0.5 - 2.0)$  are the PSPC counts collected in the 0.1-0.4 keV and 0.5-2.0 keV bands respectively. The 0.5-2.0 keV absorption-corrected flux was computed in Ceballos & Barcons (1996) by assuming a  $\Gamma = 1.9$  power law spectrum with galactic absorption, resulting in  $(1.9 \pm 0.2) \times 10^{-12}$  erg cm $^{-2}$  s $^{-1}$ .

#### 3.3 ASCA

*ASCA* observed H1320+551 on May 10 of 1999 for 10 ks. We have retrieved the pipeline-reduced data from the HEASARC public archive. The SIS0 and SIS1 data over the 0.5-8 keV band can be well fitted with a single power law with galactic absorption, resulting in a  $\chi^2 = 17.4$  for 26 degrees of freedom (see fig. 3 for the *ASCA* spectrum). The data do not require additional absorption or a soft excess.

Fig 4 shows the confidence contours for the power-law photon index ( $\Gamma = 1.53 \pm 0.1$ ) and the normalisation required by the *ASCA* data. We have also overlayed lines with various 2-10 keV flux levels, for comparison with the XMM-Newton observations. Indeed the *ASCA* 2-10 keV flux is 10 times smaller than the flux assigned to this source by the MC-LASS survey, although part of this discrepancy might be due to source confusion in the HEAO-1 data.

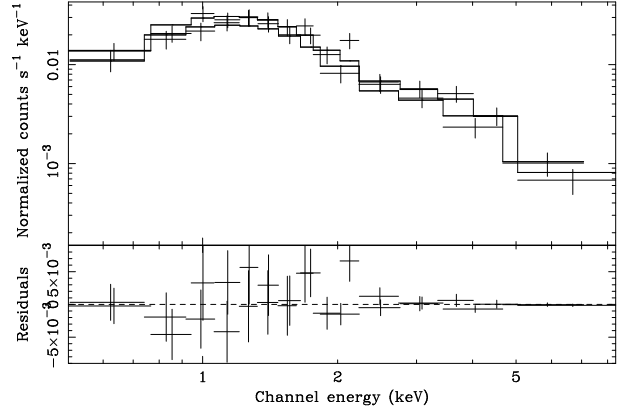


**Figure 3.** ASCA SIS0 and SIS1 spectrum of H1320+551 together with power-law fit plus Galactic absorption.

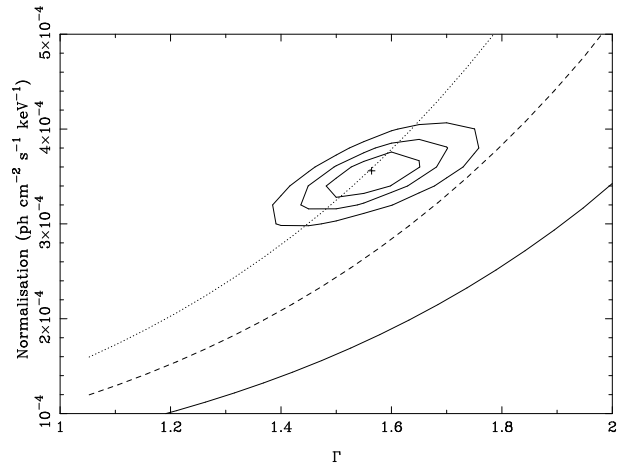


**Figure 4.** Confidence contours (1,2 and 3 sigma for 2 parameters) for the power law index and normalisation of the fit to the *ASCA* data for H1320+551. Lines at various 2-10 flux levels are also overlayed: 1.0 (continuous), 1.5 (dashed) and 2.0 (dotted)  $\times 10^{-12}$  erg cm $^{-2}$  s $^{-1}$

### 4 XMM-NEWTON X-RAY OBSERVATIONS

H1320+551 was observed by XMM-Newton (Jansen et al 2001) during revolution 366 on the 8th of December 2001. This observation was taken as part of the Guaranteed Time of the Survey Science Centre. The EPIC pn camera (Strüder et al 2001) was operated in small window mode with the Thin filter. The MOS cameras (Turner et al 2001) were operated in timing mode. The RGS spectrographs (den Herder et al 2001) were operated in standard spectroscopy mode, but our target produced a very faint signal. Due to the brightness of the source in the optical, the OM optical camera (Mason et al 2001) was switched off during this observation. In this paper we present the analysis of the EPIC pn data only, as the Science Analysis Software (SAS) version 5.3.3 provides full support for calibration matrices of the small window mode. The same version of the SAS is not meant to provide response matrices for the MOS cameras in timing mode.

The EPIC pn exposure time was 20 ks, with a count rate of 1.7 cts/s in the 0.2-12 keV band. The background did not flare significantly during the observation. We used

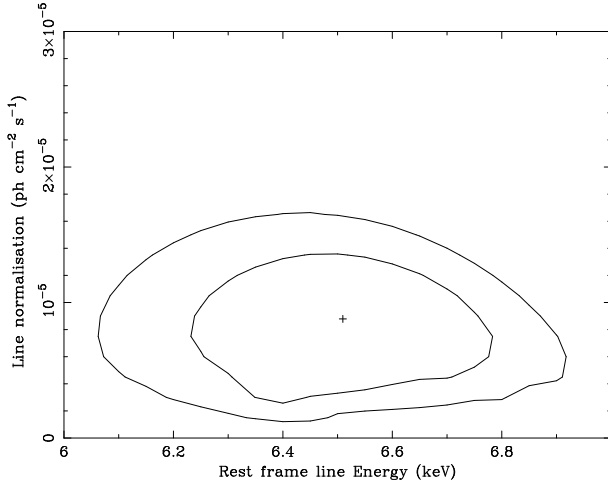


**Figure 5.** Confidence contours (1 and 2 sigma) for the rest frame Fe K line energy and intensity, following a gaussian fit.

the EPIC pn calibrated event list provided in the pipeline products, which were obtained by processing the observation data file with SAS version 5.2. To gain full support in the analysis, we extracted the source and background spectrum, and generated re-distribution matrices and ancillary response files using SAS version 5.3.3. The spectrum was also grouped in bins containing a minimum of 30 counts. All counts outside the 0.2–12. keV range were ignored.

As a first exercise, we computed the hardness ratios

$$HR_1 = \frac{S(2.0 - 4.5) - S(0.5 - 2.0)}{S(2.0 - 4.5) + S(0.5 - 2.0)} \approx -0.681$$

$$HR_2 = \frac{S(4.5 - 12.0) - S(2.0 - 4.5)}{S(4.5 - 12.0) + S(2.0 - 4.5)} \approx -0.343$$

These turn out to be entirely consistent with the average hardness ratios of the broad-line AGNs found in the AXIS medium sensitivity survey:  $\langle HR_1 \rangle = -0.68 \pm 0.01$  and  $\langle HR_2 \rangle = -0.31 \pm 0.04$  (Barcons et al 2002). The type 2 AGN in that survey have an average  $\langle HR_1 \rangle = -0.48 \pm 0.11$ , which appears marginally harder than the values for H1320+551.

#### 4.1 The 2–12 keV spectrum

We first fitted the 2–12 keV range with a single power law. We then checked for the existence of a (redshifted) Fe K line complex around 6–7 keV. A line was found at rest frame energy of  $\sim 6.5$  keV, with a very poorly defined intrinsic FWHM width of  $\sim 0.9$  keV (see Table 4.2 for the specific values). The significance of the line, as measured with the F-test statistic, is  $\sim 98\%$ . Confidence contours in the line rest frame energy and line intensity parameter space are shown in Fig 5. The corresponding equivalent width is  $\sim 380^{+230}_{-320}$  eV in the rest frame. These parameters are roughly consistent with what is expected in Compton-thin type 2 Seyferts, where multiple components of the Fe K line might be present (see, e.g., Iwasawa, Fabian & Matt 1997).

#### 4.2 The soft excess and photoelectric absorption

When this fit is extrapolated to lower energies, a large soft excess becomes evident. We model this by adding a (red-

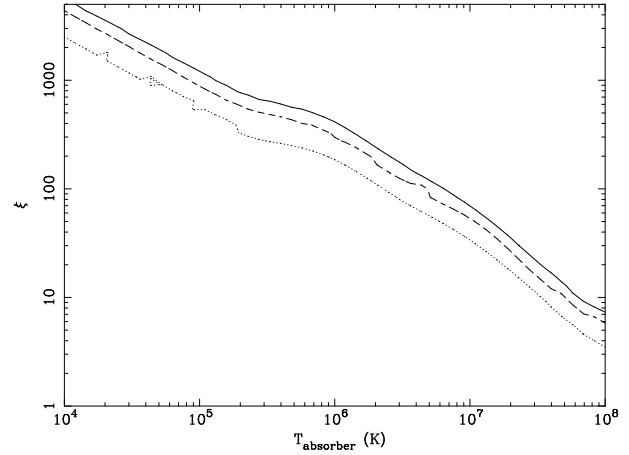


**Figure 6.** Limits for a  $N_H = 10^{22} \text{ cm}^{-2}$  ionized absorber implied by the EPIC-pn data: 1 sigma (continuous), 2 sigma (dashed) and 3 sigma (dotted).

shifted) black body, and a local photoelectric absorption to account both for the Galactic one and any possible additional absorption in the source (note that we expect this to be  $\sim 10^{22} \text{ cm}^{-2}$  based on the Balmer decrement of the BLR). The fit results in a  $\chi^2 = 439.93$  for 413 degrees of freedom and a probability of the model not being able to describe the data of only 83%. We tried to fit a plasma emission model (Raymond-Smith) instead of the black body, but no good fit could be achieved.

The rather high black body temperature ( $kT_{BB} \sim 140$  eV) suggests a low black hole mass  $M_{BH} \sim 10^4 - 10^5 M_\odot$ , which is consistent with a luminosity of  $\sim 3 \times 10^{43} \text{ erg s}^{-1}$  from such a black hole radiating at near the Eddington limit.

It is remarkable that the fit to the X-ray data does not require any photoelectric absorption in excess to the galactic value ( $N_{Gal} \sim 1.36 \times 10^{20} \text{ cm}^{-2}$ ). In fact we have frozen  $N_H$  to this value and added an extra photoelectric absorption component at the redshift of the target  $z = 0.0653$ . Re-fitting the data to this model finds its best value at no intrinsic absorption with a 3 sigma upper limit of  $1.4 \times 10^{20} \text{ cm}^{-2}$ . This value is 70 times smaller than the minimum predicted from the BLR Balmer decrement interpreted in terms of dust reddening and for a normal gas to dust ratio. It is even 7 times smaller than the value implied by the NLR reddening, but this might just be due to small covering factor of an internally reddened NLR.

The existence of an ionised absorber is ruled out by the X-ray data. The addition of a multiplicative `absori` model with a fixed column density of  $N_H \sim 10^{22} \text{ cm}^{-2}$  does not improve the  $\chi^2$ . Only very large values of the ionisation parameter  $\xi > 1000$  or very high temperatures of the absorber ( $kT \sim 10^8$  K) can reach a  $\chi^2$  as good as (but not smaller than) the one without an ionised absorber (see fig 6).

#### 4.3 Resulting spectrum

Fig 7 shows the resulting EPIC-pn spectrum after the overall fit was performed, together with the contributions to the  $\chi^2$  from each channel. There are no residuals at the energies of the most prominent absorption edges. The existence of a

Parameter	Value
Photoelectric abs:	<b>phabs</b>
$N_H$	$(1.69^{+0.45}_{-0.39}) \times 10^{20} \text{ cm}^{-2}$
Redshifted power law:	<b>zpowerlw</b>
$\Gamma$	$1.87 \pm 0.05$
$A_\Gamma$	$(7.2^{+0.5}_{-0.3}) \times 10^{-4} \text{ ph cm}^{-2} \text{ s}^{-1}$
Redshifted black body:	<b>zbody</b>
$kT$	$137^{+13}_{-12} \text{ eV}$
$A_{BB}$	$(7.1^{+1.4}_{-1.3}) \times 10^{-6}$
Redshifted Fe K line complex:	<b>zgaussian</b>
$E_{line}^*$	$6.51 \pm 0.30 \text{ keV}$
$\sigma_{line}^*$	$0.4^{+0.35}_{-0.4} \text{ keV}$
$F_{line}$	$(10.5^{+3.7}_{-4.4}) \times 10^{-5} \text{ ph cm}^{-2} \text{ s}^{-1} \text{ keV}^{-1}$

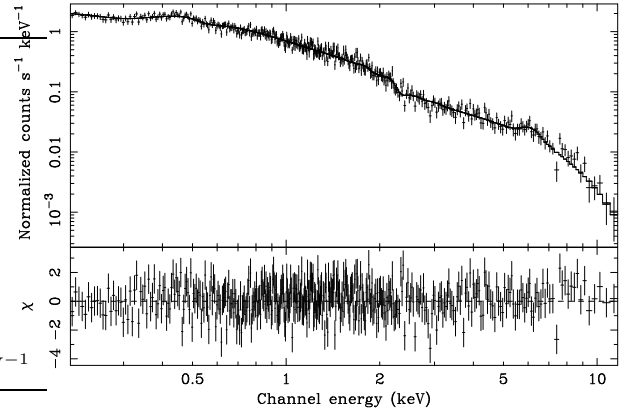
**Table 2.** Best-fit parameters for the X-ray spectrum of H1320+551 ( $z = 0.0653$  assumed throughout). Parameters are grouped by model component, and the `xspec` routine used is also listed. Errors denote the 90% interval for one parameter in each case. The best-fit values and errors have been obtained by fitting the full 0.2-12.0 X-ray spectrum shown in the text, with the exception of the parameters labelled with \* which were obtained by fitting the 2-12 keV spectrum with a redshifted power law plus a gaussian.

slight positive residual at the hard energy end is uncertain as the background level is very high at these energies.

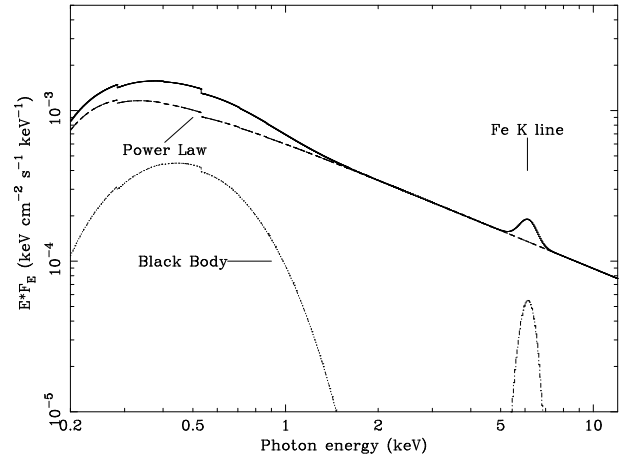
There is a negative residual at around 0.7 keV in the data (see Fig 7). The feature extends for 0.1-0.2 keV with an amplitude of  $\sim 10$  per cent. At the moment, individual calibration of the EPIC-pn instrument gives residuals of  $\sim 3$  per cent or less, but joint calibration of all XMM-Newton instruments leaves large discrepancies between EPIC pn and EPIC MOS in the energy range 0.3-1.3 keV of up to 15 per cent. Besides that, a negative residual similar to ours is seen in many EPIC-pn spectra at around 0.7 keV (S. Sembay, private communication) and therefore we believe it to be a calibration artifact.

Fig 8 shows the model fitted with the various components labelled. The flux, corrected for photoelectric absorption (assumed galactic) of the source is  $\sim 1.62 \times 10^{-12} \text{ erg cm}^{-2} \text{ s}^{-1}$  in the 0.5-2 keV band and  $2.09 \times 10^{-12} \text{ erg cm}^{-2} \text{ s}^{-1}$  in the 2-10 keV band. The luminosity is  $3.1 \times 10^{43} \text{ erg s}^{-1}$  in the 0.5-2 keV band and  $3.9 \times 10^{43} \text{ erg s}^{-1}$  in the 2-10 keV band. About 22% of the 0.5-2 keV luminosity ( $\sim 7 \times 10^{42} \text{ erg s}^{-1}$ ) is contributed by the soft excess that we have modeled as a black body, which is far too much to be attributable to the host galaxy or to scattering.

The fit to the X-ray spectrum is therefore typical of a Seyfert 1 galaxy. There is an underlying power law, to which a soft excess, probably the direct quasi-thermal radiation from the accretion disk, has to be added. The Fe K emission line complex is rather broad (FWHM  $\sim 900 \text{ eV}$ ), as it is often found in Seyfert 2 galaxies, for example in the prototypical NGC 1068 (as a result of the superposition of various components, Iwasawa et al 1997). The equivalent width of the complex is  $380^{+330}_{-320} \text{ eV}$  which lies in between the one expected from a Seyfert 1 and a Compton-thin Seyfert 2, all consistent with the Seyfert 1.8/1.9 nature of the source.



**Figure 7.** EPIC-pn X-ray spectrum together with best fit model (top) and  $\Delta\chi$  of data points to fitted model (bottom).



**Figure 8.** Fitted model, in terms of  $E F_E$  as a function of energy, showing the various components.

#### 4.4 Source variability

In order to gain further insight into the X-ray properties of this X-ray source, we have extracted its EPIC pn light curve. Time intervals have been binned in 300 s, resulting in a signal to noise of  $\sim 18$ . The background counts have been estimated from the same background subtraction region that was used to analyze the spectrum. The resulting 0.2-12 keV light curve is shown in fig 9.

The average count rate is 1.67 ct/s. However, the light curve is not consistent with a constant flux. A first glance at fig 9 reveals that 2/3 of the properly computed  $1\sigma$  error bars do not cross the horizontal fit, while only 1/3 would be expected. The  $\chi^2$  of the fit to a constant intensity is extremely poor,  $\chi^2/\nu = 341/65$ .

To estimate the rms variability, we compare the measured variance of the count rates to the variance expected from the error bars and find 5 per cent intrinsic variability on that time scale. Although small, these variations are highly significant. Note that for a  $10^5 M_\odot$  black hole, variability is expected down to scales of seconds.

The fact that the source varies brings additional support to the rejection of a Compton thick model, which would not predict short term variability.

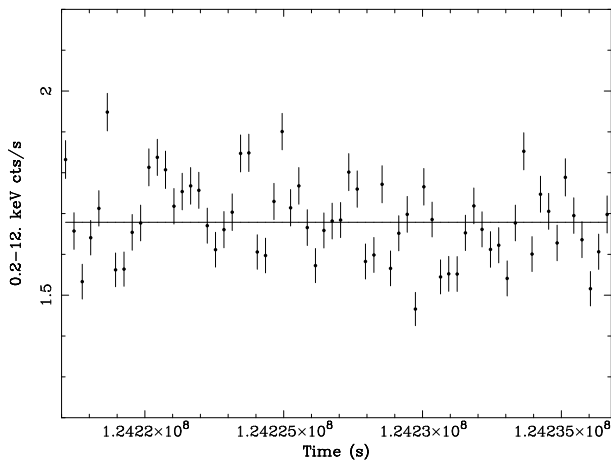


**Figure 9.** EPIC-pn X-ray light curve, binned in 300 s bins. A constant fit is shown for comparison.

## 5 DISCUSSION

Reconciling the Seyfert 1.8/1.9 character of H1320+551, as drawn from the optical observation in 1998, with the XMM-Newton data, taken late 2001, has two possible scenarios. The first one is that the source spectrum changes over time. It would then be possible that both the optical and X-ray absorbing properties change simultaneously. The other possibility is that both the optical and the X-ray properties derived from the 1998 optical data and the 2001 XMM-Newton X-ray observation stay constant over time. In that case we find that H1320+551 is not consistent with a Seyfert 1 AGN viewed through absorbing material.

### 5.1 Does the H1320+551 spectrum vary?

The first issue to address is whether the various data sets give a consistent picture of H1320+551 or there is rather strong evidence for varying spectral properties. As already discussed, the optical spectra presented here are of superior quality to that of Remillard et al (1993) and therefore we do not believe there is a strong case for claiming a change in optical spectral type from Seyfert 1 to Seyfert 1.8/1.9 by comparing the two spectra.

The HEAO-1 data gives a flux that is  $\sim 10$  times larger in the 2-10 keV band than any other reported flux in that band. Although it is entirely possible that the HEAO-1 flux was correct (therefore implying a large variation after two decades), this flux might have been severely contaminated by other sources within the same field of view of the Modulation Collimator. To further assess this point, we have searched for RASS sources in the vicinity of H1320+551, and found a total of 9 sources within a radius of 2 deg, totalling a flux  $\sim 5$  times that of our target. Although this does not prove that the HEAO-1 flux is wrong, it illustrates the difficulty in avoiding confusion problems in the MC-LASS fluxes.

The *ROSAT* all-sky survey measurement is entirely consistent with the XMM-Newton one. The 0.5-2 keV flux measured in the RASS  $((1.9 \pm 0.2) \times 10^{-12} \text{ erg cm}^{-2} \text{ s}^{-1})$  is consistent, within errors, with the 0.5-2 keV flux measured in the EPIC spectrum  $(1.6 \times 10^{-12} \text{ erg cm}^{-2} \text{ s}^{-1})$ . Furthermore, we have folded the best-fit XMM-Newton model through

the PSPC-B response and found an expected PSPC Hardness Ratio of  $+0.15$ , while  $0.12 \pm 0.10$  was measured. The spectral shape of H1320+551, as seen in the *ROSAT* and XMM-Newton observations, are entirely consistent.

The *ASCA* data give a 2-10 keV flux very similar to the XMM-Newton one, but with no soft excess visible. In fact the underlying power law in the *ASCA* data is flatter than the XMM-Newton one, with the net result that, within uncertainties, *ASCA* finds a harder spectrum than XMM-Newton. To further assess that point we simulated the *ASCA* spectrum with the model fitted to XMM-Newton. A single power law with no absorption gives a fairly acceptable fit ( $\chi^2 = 36.25$  for 26 degrees of freedom) but the power law index is significantly steeper ( $\Gamma = 2.0 \pm 0.1$ ) than the one measured in the real *ASCA* data ( $\Gamma = 1.5 \pm 0.1$ ). That discrepancy looks far too large to be attributable to cross calibration errors, which are likely to be much smaller between EPIC-pn and *ASCA* SIS (Snowden 2002). The fluxes measured in the fake *ASCA* data are 1.5 and  $1.7 \times 10^{-12} \text{ erg cm}^{-2} \text{ s}^{-1}$  in the 0.5-2 keV and 2-10 keV bands respectively, while 0.7 and  $1.65 \times 10^{-12} \text{ erg cm}^{-2} \text{ s}^{-1}$  result from the best power law fit to the real *ASCA* data. While there is agreement in the 2-10 keV band, the soft excess seen in the XMM-Newton observation, consistently with the earlier *ROSAT* observation, is not seen in the *ASCA* data.

Therefore there is some marginal evidence for X-ray spectral changes in H1320+551. Whether that implies changing absorption properties is unclear, and cannot be addressed with the archival *ASCA* observations confronted to the XMM-Newton and earlier *ROSAT* ones.

### 5.2 An intrinsic Balmer decrement

If the WHT and XMM-Newton data presented here are representative of the true average state of H1320+551, there is an apparently contradictory behaviour in the optical and in X-rays. The large Balmer decrement seen in the BLR is not consistent with the unabsorbed X-ray spectrum, if both phenomena have to be explained in terms of reddening/absorption.

Pappa et al. (2001) have studied a sample of 8 Seyfert 2 galaxies, where they find at least two without photoelectric absorption in X-rays. Three explanations were proposed in that work to account for the unusual behaviour of these sources: (a) the lack of BLR is real and intrinsic to the nuclear properties; (b) the Seyfert 2 galaxies are Compton-thick, in which case the apparent lack of photoelectric absorption would be due to the  $< 10$  keV flux coming only from scattered and/or host galaxy emission and (c) the presence of a dusty warm absorber reddens the BLR but has little effect in the X-ray properties. Indeed with the *ASCA* spectra of these objects, Pappa et al were unable to find spectral features associated to the warm absorber.

We have carefully examined these 3 possibilities in the case of H1320+551. There are two independent reasons to rule out a Compton-thick scenario (b). First we use the three-dimensional diagnostic diagram proposed by Bassani et al (1999). For H1320+551 the transmission is  $T \sim 1.5$  and the equivalent width of the Fe K line is  $\sim 400$  eV. Both numbers are inconsistent with a Compton-thick source; instead H1320+551 would be consistently placed in between the Seyfert 1s, and the Compton-thin Seyfert 2s, which is

what would be expected for a Seyfert 1.8/1.9. A second independent fact rejecting a Compton-thick scenario comes from the detection of X-ray variability on scales of 300 s. If the X-rays detected from H1320+551 were due to scattered radiation, the variability scale would be associated to the reflector rather than to the nuclear source and it would be much longer.

The possibility of a dusty warm absorber (c) is also excluded from the X-ray analysis presented here. No spectral features are detected in the X-ray data and in fact any absorbing gas present should be fully ionized, something rather inconsistent with the presence of dust reddening the BLR.

That leaves the intrinsic origin (a) for the large BLR decrement as the only likely explanation. This assumption is at odds with the standard AGN unified model and deserves some further discussion. In what follows we address the question on whether H1320+551 is consistent with an absorbed/reddened type 1 Seyfert or not.

Ward et al (1988) studied the Balmer decrement of the type 1 AGN in the Piccinotti et al (1982) sample. The good linear correlation between Balmer decrement versus the ratio between 2-10 keV luminosity (mostly unaffected by reddening/absorption) and  $H\beta$  luminosity (a good tracer of absorption) prompted Ward et al (1988) to suggest that Balmer decrement is determined by nuclear reddening, rather than being intrinsic to the BLR (see their fig. 4). They also find an approximately constant 2-10 keV to  $H\alpha$  ratio for the sample (see their Fig. 5). In fact, Ward et al (1988) conclude that in spite of the extreme conditions of the BLR, the intrinsic Balmer decrement is  $\sim 3.5$  for the type 1 AGNs.

Now, H1320+551 has a Balmer decrement which is more than half a decade larger than what would be expected from its 2-10 keV to  $H\beta$  ratio. Reddening correction will not bring this into agreement with the Seyfert 1s, as both the Balmer decrement and the X-ray to  $H\beta$  ratio will decrease if reddening corrected. On the contrary, the 2-10 keV to  $H\alpha$  ratio is entirely consistent with that of the Seyfert 1s. All that means that the large BLR decrement for this particular Seyfert 1.8/1.9, together with its unabsorbed X-ray spectrum cannot be explained as a Seyfert 1 AGN viewed through obscuring material.

### 5.3 Conclusion

XMM-Newton X-ray observations of the H1320+551, which is classified by its optical spectrum as a type 1.8/1.9 AGN, reveal no absorption. If the non-simultaneous optical and X-ray observations both trace the true state of this source, we conclude that the large Balmer decrement of the BLR, which determines its 1.8/1.9 spectroscopic type, is not due to reddening by dusty absorbing material along the line of sight. A variety of models can explain a large intrinsic value of the Balmer decrement, among them the failure of the standard “case B recombination” and/or optically thick BLR clouds. In any case, the AGN unified model fails completely in this source.

Regardless on whether the unusual optical/X-ray absorption properties of H1320+551 are due to variations or not, they raise an important issue for unified AGN models for the X-ray background. H1320+551 is a source with a relatively soft unabsorbed X-ray spectrum that is expected to

typically have a type 1 AGN optical counterpart. However, we identify it with a Seyfert 1.8/1.9, breaking again the one-to-one identification between X-ray absorption and optical obscuration that the XRB models use. Similarly, other relatively soft X-ray sources with no X-ray absorption might have optical counterparts which deviate from the standard Seyfert 1 character. If the BLR properties are not always linked to the absorption displayed by AGN, then Seyfert 1.8/1.9/2 galaxies might appear as optical counterparts of soft X-ray selected sources as well as type 1 Seyferts often appear as optical counterparts to hard X-ray sources.

### ACKNOWLEDGMENTS

We are grateful to Steve Sembay and Martin Turner for help with EPIC calibration issues. The referee is also thanked for important suggestions on the original version of this paper. The WHT telescope is operated on the island of La Palma by the Isaac Newton Group of Telescopes in the Spanish Observatorio del Roque de Los Muchachos of the Instituto de Astrofísica de Canarias. Partial financial support for this work was provided by the Spanish Ministry of Science and Technology under project AYA2000-1690.

### REFERENCES

- Alonso-Herrero A., Ward M.J., Kotilainen J.K., 1997, MNRAS, 288, 977
- Antonucci R., 1993, ARAA, 31, 473
- Baldwin J.A., Phillips M.M., Terlevich R.J., 1981, PASP, 93, 5
- Barcons X., Carrera F.J., Watson M.G. et al, 2002, A&A, 382, 522
- Bassani L., Dadina M., Maiolino R., Salvati M., Risaliti G., Della Ceca R., Matt G., Zamorani G., 1999, ApJ, 121, 473
- Bohlin R.C., Savage B.D., Drake J.F., 1978, ApJ, 224, 132
- Branduardy-Raymont G., Sako M., Kahn S.M., Brinkman A.C., Kaastra J.S., Page M.J., 2001, A&A, 365, L140
- Ceballos M.T., Barcons X., 1996, MNRAS, 282, 493
- Coleman G.D., Wu C.C., Weedman D.W., 1980, ApJS, 43, 393
- Comastri A., Setti G., Zamorani G., Hasinger G., 1995, A&A, 296, 1
- D., Cox D.P., 1972, ApJ, 177, 855
- den Herder, J.W. et al 2001, A&A, 365, L7
- Francis P.J., Hewett P.C., Foltz C.B., Chafee F.H., Weymann R.J., Morris S.L., 1991, ApJ, 373, 465
- Fiore F., La Franca F., Giommi P., Elvis M., Matt G., Comastri A., Molendi S., Gioia I., 1999, MNRAS, 306, L55
- Gilli R., Salvati M., Hasinger G., 2001, A&A, 366, 407
- Granato G.L., Danese L., Franceschini A., 1997, MNRAS, 286, 147
- Iwasawa K., Fabian A.C., Matt G., 1997, MNRAS, 289, 443
- Jansen F.A. et al, 2001, A&A, 365, L1
- Lee J.C., Ogle P.M., Canizares C.R., Marshall H.L., Schulz N.S., Morales R., Fabian A.C., Iwasawa K., 2001, ApJ, 554, L13
- Lehmann I., Hasinger G., Schmidt M. et al, 2001, A&A, 371, 833
- Mason K.O., Carrera F.J., Hasinger G., et al, 2000, MNRAS, 311, 456
- Mason, K.O. et al, 2001, A&A, 365, L36
- Nandra K., Pounds K.A., 1994, MNRAS, 268, 405
- Osterbrock, D.E., 1989, *Astrophysics of Gaseous Nebulae and Active Galactic Nuclei*, Univ Science Books, Mill Valley, California
- Page M.J., Mittaz J.P.D., Carrera F.J., 2000, MNRAS, 318, 1073
- Page M.J., Mittaz J.P.D., Carrera F.J., 2001, MNRAS, 325, 575



- Pappa A., Georgantopoulos I., Stewart G.C., Zezas A.L., 2001, MNRAS, 326, 995
- Piccinotti G., Mushotzky R.F., Boldt E.A., Holt S.S., Marshall F.E., Serlemitsos P.J., Shafer R.A., 1982, ApJ, 253, 485
- Remillard R.A., Bradt H.V., Brissenden R.J.V., Buckley D.A.H., Roberts W., Schwartz D.A., Stroozas B.A., Tuohy I.R., 1993, AJ, 105, 2079
- Risaliti G., Maiolino R., Salvati M., 1999, ApJ, 522, 157
- Savage B.D., Mathis J.S., 1979, ARAA, 17, 73
- Schwope A.D., Hasinger G., Lehmann I. et al, 2000, Astr. Nachr., 321, 1
- Setti G., Woltjer L., 1989, A&A, 224 L21
- Smith D., Done C., 1996, MNRAS, 280, 355
- Snowden S., 2002, In: New visions of the X-ray Universe in the XMM-Newton and Chandra era, F.A. Jansen ed., in the press.
- Strüder, L. et al, 2001, A&A, 365, L18
- Turner M.J.L. et al, 2001, A&A, 365, L27
- Ward M.J., Done C., Fabian A.C., Tennant A.F., Shafer R.A., 1988, ApJ, 324, 767
- Wood K.S., Meekins J.F., Yentis D.J. et al, 1984, ApJS, 56, 507

This paper has been produced using the Royal Astronomical Society/Blackwell Science L<sup>A</sup>T<sub>E</sub>X style file.